



Published in final edited form as:

Brain Res. 2020 November 01; 1746: 146987. doi:10.1016/j.brainres.2020.146987.

Comparison between Midline and Lateral Fluid Percussion Injury in Mice Reveals Prolonged but Divergent Cortical Neuroinflammation

Kristina G. Witcher^{a,d,*}, Julia E. Dziabis^{a,d,*}, Chelsea E. Bray^{a,d}, Alan J. Gordillo^{a,d}, Julia E. Kumar^{a,d}, Daniel S. Eiferman^b, Jonathan P. Godbout^{a,c,d}, Olga N. Kokiko-Cochran^{a,c,d,e}

^aDepartment of Neuroscience, The Ohio State University, 333 W 10th Ave, Columbus, OH 43210, USA

^bDepartment of Surgery, The Ohio State University, 395 W 12th Ave, Columbus, OH 43210, USA

^cCenter for Brain and Spinal Cord Repair, The Ohio State University, 460 W 12th Ave, Columbus, OH 43210, USA

^dInstitute for Behavioral Medicine Research, The Ohio State University, 460 Medical Center Dr, Columbus, OH 43210, USA

Abstract

Animal models are critical for determining the mechanisms mediating traumatic brain injury-induced (TBI) neuropathology. Fluid percussion injury (FPI) is a widely used model of brain injury typically applied either midline or parasagittally (lateral). Midline FPI induces a diffuse TBI, while lateral FPI induces both focal cortical injury (ipsilateral hemisphere) and diffuse injury (contralateral hemisphere). Nonetheless, discrete differences in neuroinflammation and neuropathology between these two versions of FPI remain unclear. The purpose of this study was to compare acute (4–72 hours) and subacute (7 days) neuroinflammatory responses between midline and lateral FPI. Midline FPI resulted in longer righting reflex times than lateral FPI. At acute time points, the inflammatory responses to the two different injuries were similar. For instance, there was evidence of monocytes and cytokine mRNA expression in the brain with both injuries acutely. Midline FPI had the highest proportion of brain monocytes and highest IL-1 β /TNF α mRNA expression 24 h later. NanoString nCounter analysis 7 days post-injury revealed robust and prolonged expression of inflammatory-related genes in the cortex after midline FPI compared to lateral FPI; however, Iba-1 cortical immunoreactivity was increased with lateral FPI.

^oTo whom correspondence should be addressed: O.N. Kokiko-Cochran, 257 IBMR Bldg., 460 Medical Center Dr, The Ohio State University, Columbus, OH 43210, USA; Tel: (614) 366-3642, Olga.Kokiko-Cochran@osumc.edu.

*Authors contributed equally.

Credit Author Statement: KGW and JED performed surgeries and injuries for midline fluid percussion injury, assisted with all data analysis, and wrote the manuscript; CEB assisted with gene expression and immunohistochemical analysis; AJG assisted with immunohistochemical analysis; JEK assisted with immunohistochemical analysis; DSE provided expertise in brain injury and inflammation and edited the manuscript; JPG provided expertise in brain injury and inflammation and edited the manuscript; OKC performed surgeries and injuries for lateral fluid percussion injury, assisted with data analysis, and wrote the manuscript.

Publisher's Disclaimer: This is a PDF file of an unedited manuscript that has been accepted for publication. As a service to our customers we are providing this early version of the manuscript. The manuscript will undergo copyediting, typesetting, and review of the resulting proof before it is published in its final form. Please note that during the production process errors may be discovered which could affect the content, and all legal disclaimers that apply to the journal pertain.

Declarations of interest: None

Thus, midline and lateral FPI caused similar cortical neuroinflammatory responses acutely and mRNA expression of inflammatory genes was detectable in the brain 7 days later. The primary divergence was that inflammatory gene expression was greater and more diverse subacutely after midline FPI. These results provide novel insight to variations between midline and lateral FPI, which may recapitulate unique temporal pathogenesis.

Keywords

Traumatic brain injury; Fluid percussion injury; Neuroinflammation; Microglia

1. Introduction

Traumatic brain injury (TBI) is a leading cause of morbidity and mortality worldwide, with approximately 6 million Americans living with the chronic effects of head injury (Faul et al., 2010). TBI, defined as brain damage resulting from an external mechanical force to the head, causes both acute and chronic complications. Inflammatory processes are implicated in both acute and chronic pathology after TBI (Cherry et al., 2016; Fenn et al., 2014; Ramlackhansingh et al., 2011). Therefore, it is important to understand how the acute inflammatory processes immediately following injury can, when unresolved, progress into a maladaptive and damaging response.

Animal models of injury are critical to understanding the molecular mechanisms mediating inflammatory responses to TBI. Fluid percussion injury (FPI) is one of the most common experimental TBI models (Lyeth, 2016). A fluid pulse is directly applied to the dura mater of rodents to induce behavioral symptomology and neuropathology consistent with human injury (Cortez et al., 1989; Lifshitz et al., 2016). FPI is commonly applied at midline or parasagittal to midline (lateral). Midline FPI induces a diffuse TBI, with bilateral structural injury and inflammation. Lateral FPI is a mixed model of TBI; the ipsilateral hemisphere receives a focal cortical injury and both subcortical and contralateral structures are diffusely injured. This is a necessary broad description because specific brain coordinates for the exact location of injury do vary between laboratories. Nonetheless, the primary distinction between midline FPI and lateral FPI is the position of the craniectomy, which produces a bilateral or unilateral TBI, respectively.

Despite the prevalence of FPI in modeling TBI, few direct comparison studies are published. Grady et al. (2003) compared neuronal loss and microglial proliferation in the rat hippocampus following midline and lateral FPI at 14 dpi. Midline FPI was administered 2 mm caudal to bregma. Lateral FPI was administered 2 mm caudal to bregma and 2 mm right of the sagittal suture. They found increased neuronal loss in the hippocampus ipsilateral to lateral FPI compared to naïve controls, however there was no significant loss of neurons in midline FPI or contralateral hemispheres after lateral FPI. Furthermore, they found increased numbers of microglia in the ipsilateral hippocampus after lateral FPI compared to midline FPI and controls 14 dpi. This analysis was limited to one time-point and determination of cell-type by nuclear size, rather than cell-type specific immunolabeling. Nonetheless, their

findings support the idea that lateral FPI induces a more profound injury with neuronal loss compared to midline FPI.

The purpose of this study was to compare midline and lateral FPI and identify discrete differences in acute and subacute inflammation. Midline FPI induces a diffuse injury and is characterized by widespread axonal injury in the absence of a focal contusion (Dixon et al., 1987; Lifshitz et al., 2016). The contralateral hemisphere undergoes similarly widespread, diffuse injury forces following lateral FPI (Cortez et al., 1989). In contrast, cortical herniation through the dura mater causes a focal contusion in the ipsilateral cortex following lateral FPI (Carbonell and Grady, 1999). Thus, we sought to compare whether the magnitude of inflammation following these injuries in mice mirrored established histopathology reported in rats (Grady et al., 2003). Notably, a smaller craniectomy is performed in mice (3 mm diameter) compared to rats (4 mm diameter) for FPI. Thus, midline FPI or sham injury was applied -0.5 to -3.5 mm from bregma and midpoint along the sagittal suture. Lateral FPI or sham injury was applied -0.5 to -2.5 mm from bregma and midpoint 2.5 mm lateral to the sagittal suture. We hypothesized that acute inflammatory responses (immune cell trafficking, cytokine mRNA expression) would be enhanced in the ipsilateral hemisphere after lateral FPI compared to the contralateral hemisphere after lateral FPI and both hemispheres after midline FPI in mice. We also predicted that the ipsilateral cortex after lateral FPI would have a similarly protracted inflammatory state in the sub-acute period 7 dpi.

2. Results

2.1 Midline FPI induces prolonged righting reflex but similar acute inflammatory response compared to lateral FPI.

We compared the acute and sub-acute inflammatory responses to midline and lateral FPI (Fig.1A–B). Mice received midline or lateral FPI (Fig.1A) and time to self-right was measured immediately after injury. There was a main effect of injury on time to self-right ($F_{1,37}=51.15$; $p < 0.0001$) and an interaction between craniectomy location and injury ($F_{1,37}=7.24$; $p < 0.01$, Fig.1C). While there was no difference between midline and lateral sham controls, both midline and lateral FPI caused increased righting times. Furthermore, mice took the longest to self-right after midline FPI compared to all other groups ($p < 0.05$). Thus, despite identical injury parameters, including time of day and pressure applied, midline FPI induces a longer time to self-right than lateral FPI.

Next, we sought to determine if midline and lateral FPI differentially induced peripheral myeloid cell trafficking to the brain at acute time-points post-injury. The greatest percentage of CD11b⁺/CD45^{hi} myeloid cells was observed 4 hours post- (hpi) injury and was lowest 72 hpi (Fig.1D). At 4 hpi, there was a main effect of injury on infiltrating myeloid cells ($F_{1,23}=13.13$, $p < 0.05$). Post-hoc analysis revealed a significant increase in infiltrating cells in ipsilateral hemisphere after lateral FPI ($p < 0.05$). At 24 hpi, there was a significant interaction between location and injury ($F_{2,22}=9.82$, $p < 0.05$) and a main effect of injury ($F_{1,22}=23.42$, $p < 0.001$). While myeloid cell percentage remained elevated 24 h in ipsilateral hemisphere after lateral FPI compared to sham-controls, midline FPI induced the greatest percentage of infiltrating myeloid cells. At 72 hpi, there was a trending effect of

injury location ($F_{1,22}=22.62$, $p < 0.06$), but no significant differences between groups. Collectively, FPI induces transient acute myeloid cell infiltration that is greatest in ipsilateral hemisphere after lateral FPI and lowest in contralateral hemisphere after lateral FPI.

From the same mice, a coronal brain section -1 to -2 mm from bregma was used to determine mRNA expression of the inflammatory cytokines IL- 1β and TNF α (Fig.1E). As before, brain sections were bisected to differentiate ipsilateral and contralateral hemispheres after lateral FPI and left intact following midline FPI. There was a significant interaction between injury type and TBI at 24 h on *Il1b* gene expression ($F_{2,22}=20.14$, $p < 0.05$), with midline FPI inducing the greatest increase in expression ($p < 0.05$). *Tnf* expression was similarly induced by midline FPI at 4 h and 24 h compared to sham-controls ($p < 0.05$). Thus, acute inflammatory cytokine expression after FPI was similar to acute myeloid cell trafficking and was increased acutely, but returned to baseline by 72 hpi.

2.2 Lateral FPI causes greater cortical lesion volume and microglial morphological shift compared to midline FPI

We next compared the sub-acute effects of midline and lateral FPI 7 dpi. Red outline identifies the damaged cortical tissue in representative photomicrographs of a coronal brain slice near bregma -2 mm (Fig.2A). First, we measured lesion area and found no significant main effects of injury or injury location at selected coordinates across the length of the brain (Fig.2B); however, there was a trending increase in total lesion volume (mm^3) between mid-TBI and lat-TBI ($p = 0.07$, Fig.2C). Next, we quantified the percent area of Iba1 labelling as well as the number of Iba1+ cells in a 20 X image of the right primary somatosensory cortex in two coronal brain slices near bregma -2 mm. We observed a main effect of injury ($F_{1,22}=38.79$, $p < 0.01$), with the greatest Iba1+ area in ipsilateral cortex after lateral FPI ($p < 0.05$, Fig.2D–E), however there were no statistically significant changes in total number of Iba1+ cells (Fig.2F–G).

2.3 Midline FPI exaggerates cortical inflammatory gene expression compared to lateral FPI 7 DPI.

To determine if these changes in cortical loss and microglial/macrophage reactivity correlated with inflammation, we used a NanoString nCounter mouse inflammation panel to compare gene expression after midline and lateral FPI. Specifically, the cortex from the right brain hemisphere was dissected after midline or lateral FPI or sham injury. Principle component analysis determined overall sources of variance describing the dataset (Fig.3A). There was a main effect of TBI in the first principle component ($F_{1,22}=24.99$, $p < .01$). Heatmap of select genes shows average gene expression of microglia signature genes and genes related to chemokine, interferon, cytokine, and complement signaling (Fig.3B). While microglial signature genes were elevated in both FPI groups (*Cx3cr1*, *Trem2*, *Tgfbr1*), midline FPI induced the greatest increases in inflammatory chemokine (*Ccl2*, *Ccl5*) and cytokine responses (*Ifi44*, *Il1b*, *Il6*) compared to sham injured controls. Together these findings suggest that while lateral FPI causes increased cortical tissue loss and structural microgliosis, midline FPI induces greater persistent changes in inflammatory gene expression.

3. Discussion

This study sought to elucidate the differences in acute and subacute inflammation between two widely used models of experimental TBI: midline and lateral FPI. We compared diffuse cortical injury (midline FPI) to focal cortical injury (lateral FPI) in mice. In lateral FPI, a fluid pulse is applied directly to the parietal cortex, causing dural disruption over the parietal cortex and subsequent herniation through the craniectomy. In contrast, midline FPI indirectly injures the parietal cortex through coup-contrecoup movement of the brain within the skull. While the medial cortex is under the fluid pulse, dural integrity is maintained and there is no gross anatomical deformity. We predicted that lateral FPI, which results in focal cortical injury, would produce more severe inflammatory responses than midline FPI. Thus, we measured leukocyte trafficking to the brain and acute inflammatory cytokine induction acutely (4–72 hpi) and measured microglial immunoreactivity and cortical gene expression subacutely (7 dpi).

Before discussing the inflammatory consequences, it is important to highlight differences observed immediately after injury in length of time to self-right. Both midline FPI and lateral FPI caused extended righting reflex times compared to sham controls, however midline FPI resulted in significantly longer times than lateral FPI. Notably, our findings in mice differ from previously reported data in rats, which showed no difference in self-righting times after midline and lateral FPI (Grady et al., 2003). Our findings of extended righting times after midline FPI compared to lateral FPI persisted across two separate experiments in which FPI was delivered on the same device, alternating between midline and lateral craniectomy sites. Therefore, we attribute this to anatomical differences in injury force, with midline FPI causing more mechanical impact to the brainstem at the time of primary injury (Kabadi et al., 2010; McIntosh et al., 1987).

We initially hypothesized that lateral FPI would result in more severe acute inflammatory responses, however our data contradicted this hypothesis. We did not observe differences in acute leukocyte trafficking to the ipsilateral hemisphere after lateral FPI or midline FPI. This is remarkable as cortical lesion formation in TBI is accompanied by blood-brain-barrier breakdown (Fukuda et al., 1995). Midline FPI is not accompanied by frank disruption of the blood-brain-barrier, however we previously reported that leukocytes are transiently present in the cortex after midline FPI (Fenn et al., 2015). It is possible that these cells adhere to brain endothelial cells without extravasating. These similarities in leukocyte adhesion mirrored expression of the inflammatory cytokines IL-1 β and TNF α . As previously described, these cytokines increase acutely following midline FPI and decrease by 72 hpi (Fenn et al., 2014). We hypothesized that elevated leukocyte recruitment would augment this expression in the ipsilateral hemisphere following lateral FPI. Both lateral and midline FPI induced transient changes that returned to baseline. Thus, midline and lateral FPI induce similar cortical inflammatory responses in the acute phase.

Importantly, the side contralateral to the lateral FPI craniectomy and injury exhibited the lowest levels of inflammation in our acute studies. Therefore, we used the contralateral side of sham-controls to normalize our rt-PCR analysis of *Illb* and *Tnf* gene expression. This revealed a significant effect of sham-surgery alone on inflammatory gene expression in both

midline and ipsilateral FPI conditions. Brain-associated leukocyte populations (CD11b⁺/CD45^{hi} cells) observed in the 4 hour time point appear elevated compared to 72 hpi. Because these were performed as separate experiments and without naïve controls, these values cannot be directly compared. Nonetheless, there is a modest inflammatory response to craniectomy alone, and exposure of the dura presents some superficial trauma to the brain. The use of sham-operated controls presents a limitation in the field of TBI and has been previously discussed (Cole et al., 2011). While surgical controls induce some brain inflammation, we observed robust inflammatory changes following both midline and lateral FPI.

As predicted, lateral, but not midline, FPI enhanced cortical tissue loss. We observed high variability in lesion volume between mice after lateral FPI, which prevented the analysis from reaching statistical significance. Notably, variability in lesion size is not uncommon following lateral FPI, and previous studies confirm that even small shifts (i.e., 1mm) in craniectomy position are associated with differences in lesion size (Vink et al., 2001). We also observed some region-specific cortical damage following surgical preparation in lateral sham injured mice. This is consistent with recent reports showing that even careful sham surgeries from an experienced surgeon can result in quantifiable structural and biochemical damage. Nonetheless, no lesion development (< 0.1mm³) occurred following mid-FPI, with less variability in sham tissue loss. Together, these data suggest that the underlying brain tissue is more vulnerable to damage during surgical preparation for lateral FPI than midline FPI.

Despite similarities in acute injury responses, inflammatory responses diverged in the subacute (7 dpi) phase post-injury. While lateral FPI induced greater Iba1⁺ percent-area suggestive of morphological changes in reactive microglia, midline FPI showed greater inflammatory gene expression responses compared to controls. Both midline and lateral FPI caused increased expression of characteristic microglial genes, including *C3ar1*, *Tyrobp*, *Tgfb1*, and *H2-Eb1*. Elevated MHC-II expression (*H2-Eb1*) is implicated in microglial priming to subsequent immune challenge (Fenn et al., 2014), thus both injuries may also cause microglial priming. Importantly, midline FPI alone caused significant increases in chemokines (*Ccl2*, *Ccl5*), interferon responsive genes (*Ifi44*, *Ifi2712a*), and cytokines (*Il1b*, *Il1a*) compared to corresponding sham controls. This suggests a difference in the progression of injury over time. Lesion formation (Schurman et al., 2017) and microglial morphological change do not necessarily correlate with inflammation. It is possible that scar tissue proximal to the lesion effectively resolved inflammation from the focal primary insult in lateral FPI, whereas diffuse injury after midline FPI continued to evolve over time. Previous reports suggest injured neurons persist in the cortex after midline FPI, rather than undergoing apoptosis/necrosis at the time of injury (Greer et al., 2011). Nonetheless, focal (lateral FPI) and diffuse (midline FPI) induce divergent subacute inflammatory responses in mice.

Understanding the differences between the kinetics and nature of post-injury inflammation between focal and diffuse rodent models of TBI is critical to furthering our understanding of post-brain trauma pathology. Because inflammation is a primary target of many pre-clinical therapeutics, these differences likely influence therapeutic efficacy and translation. Human

brain injury is heterogeneous clinically, therefore it is important that preclinical models cover this spectrum. Here, we show that inflammatory gene expression in the cortex persists in midline FPI but either resolves or is different in nature 7 days after lateral FPI. Thus, anti-inflammatory therapeutic strategies may change in efficacy depending on the nature of TBI. Indeed, recent studies using a small-molecule therapy that attenuates IL-1 β production after injury showed differing efficacy between closed-head injury and midline FPI (Bachstetter et al., 2015; Bachstetter et al., 2016). Recent efforts by the Transforming Research and Clinical Knowledge (TRACK)-TBI consortium have begun systematically collecting imaging and biomarker data from thousands of TBI patients in order to improve translation of therapeutics across diverse clinical presentations.

Collectively, our findings suggest that midline FPI and lateral FPI share acute inflammatory features, but have divergent sub-acute inflammatory responses in the cortex. These results are in line with previous publications demonstrating that craniectomy location produces unique pathogenesis but further emphasizes the temporal component of these differences soon after injury. Additional studies are needed to define the chronic inflammatory response at multiple post-injury time points. It is possible that the secondary injury cascade following midline and lateral FPI differentially affects sub-cortical structures and behavioral recovery in a distinct temporal progression. These seemingly subtle neuroinflammatory differences between midline and lateral FPI may have striking consequences in recovery and justify the use of one model over the other in future studies.

4. Experimental Procedure

4.1 Subjects

Equal numbers of male and female adult C57BL/6 mice (8–10 weeks; Charles River Laboratories). Mice were group-housed by sex in The Ohio State University's Wiseman Hall vivarium and maintained at 21°C under a 12h light/12h dark cycle (i.e., lights on 7AM–7 PM) with *ad libitum* access to food and water. All procedures followed the NIH Guidelines for Care and Use of Laboratory Animals and were approved by The Ohio State University IACUC.

4.2 Surgical preparation and injury

Briefly, mice were anesthetized with 4% isoflurane for 4 minutes and then positioned in a stereotaxic frame. After a midline incision, a 3mm craniectomy was performed –0.5 to –3.5 mm from bregma and midpoint along the sagittal suture (midline FPI) or –0.5 to –2.5 mm from bregma and midpoint 2.5 mm lateral to the sagittal suture (lateral FPI; Fig. 1A) with careful attention to leaving the dura matter intact. A modified portion of a Leur-Loc (3mm inner diameter) was positioned over the exposed dura and secured with cyanoacrylate adhesive. Surgeries began at 7AM and were completed by 12PM. Afterward, all mice were returned to their home cage where they recovered overnight. Approximately 24 hours after the surgical procedure, mice were anesthetized with 4% isoflurane for 4 minutes and then connected to the FPI device (Custom Design & Fabrication, Richmond, VA). TBI or sham injury was performed as previously described (Fenn et al., 2014; Kokiko-Cochran et al., 2018). A fluid pulse was used to create the TBI at a magnitude of 1.2 atm of pressure as

previously described (Witcher et al., 2018). The Leur-Loc and adhesive were removed before time to self-right was recorded. Mice recovered on a heating pad before being returned to their home cage. All injuries were performed in the morning from approximately 9–11 AM. Separate cohorts of 24 mice (N = 6 midline FPI, N = 6 midline sham, N = 6 lateral FPI, N = 6 lateral sham) were sacrificed at 4, 24, and 72 hours and 7 days after FPI or sham injury. Equal numbers of male and female mice (N = 3) were included in each experimental group.

4.3 Preparation of brain tissue for analysis

At 4, 24, and 72 hpi, we removed a 1mm coronal brain slice using a mouse brain matrix from the area under the craniectomy site at approximately –1 to –2 mm from bregma from each mouse. We then bisected this coronal slice into ipsilateral/contralateral from lateral FPI mice or kept intact (midline FPI) prior to flash-freezing. The remaining brain was then bisected or kept intact for brain homogenization/Percoll gradient separation for flow cytometry. The primary injury is localized to the ipsilateral hemisphere during lateral FPI; however, the contralateral hemisphere displays a contrecoup response to the initial insult. Because we expected a unique ipsilateral and contralateral response following lateral FPI, the brains were bisected prior to analysis. The primary injury is applied along the central suture during midline FPI, which should theoretically affect both hemispheres equally. Because we expected the right and left brain hemispheres to be similarly affected by midline FPI, the brains were not bisected prior to analysis. To control for differences in brain volume, we were careful to present data as relative to a housekeeping gene or stable cell population. In this case, more sample does not skew results. At 7 dpi, separate cohorts of mice were used for NanoString and immunohistochemical analysis. Specifically, the right cortex was microdissected for NanoString and coronal brain slices were used for image analysis.

4.4 Percoll-enrichment of CD11b⁺ cells and flow cytometry

At 4, 24, and 72 h after FPI (Fig.1B), brain immune cells were enriched as previously described (Fenn et al., 2014). In brief, single-cell suspensions were generated from whole brains and layered on a discontinuous Percoll density gradient (GE-Healthcare). Enriched microglia/brain leukocytes were collected from the 50–70% interface and used for flow cytometric analysis. Cells were labeled with fluorochrome-conjugated primary antibodies (1:50; CD45-PerCP-Cy5.5, CD11b-APC, eBiosciences). Surface receptor expression was determined using a custom Becton-Dickinson FACSCalibur cytometer and analyzed with FlowJo software.

4.5 Gene expression assay

At 4, 24, and 72 h after FPI (Fig.1B), brain tissue was removed and 1mm thick coronal sections were collected using a brain matrix (Ted Pella, Inc.). Sections were bisected following lateral FPI into ipsilateral and contralateral hemispheres. Brain sections/hemisectons were snap-frozen and RNA was isolated using TriReagent per manufacturer protocols (Sigma-Aldrich). RNA (1.2µg per sample) was reverse-transcribed (HiCap RT-PCR kit, Applied Biosystems) and quantitative real-time (qRT)-PCR was performed using the Applied Biosystems Taqman Gene Expression protocol. Data were analyzed using the

comparative threshold method ($\Delta\Delta Ct$) and normalized to *Gapdh* expression and reported as fold change from time-matched contralateral-sham controls.

At 7 DPI, half of mice in each experimental group were used for NanoString analysis. Briefly, the cortex from the right hemisphere after midline or lateral FPI or sham injury was microdissected, snap frozen, and RNA was extracted as described above. The NanoString nCounter Mouse Inflammation panel was used to quantify expression copy number. To account for batch effects caused by using midline and lateral samples from separate experiments, empirical housekeeping genes were determined based on strong positive correlation with total counts ($R^2 > 0.95$). Samples were normalized to housekeeping expression using DESeq2 (Love et al., 2014) and visualized using heatmap in R.

4.6 Lesion Analysis and Immunofluorescence

At 7 DPI, half of the mice in each group, including midline or lateral FPI and corresponding sham injury were used for histology. Briefly, mice were perfuse-fixed with 4% paraformaldehyde, brains were post-fixed, dehydrated, and cryosectioned. For lesion analysis, sections at 10 coordinates were stained with DAPI, fluorescent tilescan images were taken of each section, and lesion area at each coordinate was measured by a blinded investigator. For analysis of microglia, sections were blocked (5% normal donkey serum, 5% bovine serum albumin, 0.1% TritonX) and incubated with primary antibodies against Iba1 (1:1000, Wako Chemicals) followed by secondary antibodies (1:500, AlexaFluor 594, Invitrogen). Fluorescent images were taken with an EVOS FL Auto 2 imaging system (Thermo Fisher) at 20X magnification. Counts of Iba1+ cells were quantified using ImageJ Software (NIH) by investigators blinded to experimental group. Images were converted to greyscale 8-bit format and noise despeckle and subtract background (rolling ball radius: 50.0 pixels) processes were applied. Threshold was then adjusted to fill cell bodies. Particle analysis was conducted with a minimum size requirement of 150 pixels². Values from 4–5 images were averaged for each mouse. Mouse averages were then used to determine averages and variance for each experimental group. Percent-area of Iba1 labeling was also quantified with ImageJ Software (NIH). Values from 4–5 images were averaged for each mouse; mouse averages were then used to calculate averages and variance for each experimental group. Investigators were blinded to injury throughout analysis.

4.7 Statistical analysis

The primary objective of this study was to define the inflammatory response to FPI and compare inflammatory changes between midline and lateral positioning of the TBI with respective sham control mice at acute and sub-acute post-injury time points. This resulted in a 2 (sham, TBI) x 2 (midline, lateral) x 4 (4 hours, 24 hours, 72 hours, 7 days) factorial design with separate cohorts of mice sacrificed at each post-injury time point. To determine significant effects and interactions, data were analyzed using GraphPad Prism 6 statistical software, using Two-Way ANOVA followed by Fisher *post-hoc* test to determine significant differences between group means. Main effects of injury and position of injury were determined statistically significant when $p < 0.05$. The heatmap for NanoString analysis represents pairwise comparisons using DESeq in R. Sex was not included as a primary independent variable. All data are presented as group mean \pm SEM.

Acknowledgements:

This research was supported by an NINDS R56-NS-090311 (to JPG), a College of Medicine Dean's Discovery Grant (to JPG), funding from the OSU Center for Brain and Spinal Cord Repair (to JPG), and a Chronic Brain Injury Pilot Award (to OKC). In addition, this work was supported by a P30 Core grant (NINDS P30-NS-045758). KGW was supported by a National Institute of Dental and Craniofacial Research Training Grant (T32-DE-01-4320) and an Ohio State University Presidential Fellowship. JED was supported by Ohio State's Second-year Transformational Experience Program Fellowship. The authors thank Zoe Tapp for assistance with histology, John Velasquez for surgical assistance, as well as the Chronic Brain Injury Discovery Themes Initiative at The Ohio State University.

Abbreviations:

TBI	traumatic brain injury
FPI	fluid percussion injury
dpi	days post-injury
hpi	hours post-injury

References

- Bachstetter AD, Webster SJ, Goulding DS, Morton JE, Watterson DM, Van Eldik LJ, 2015 Attenuation of traumatic brain injury-induced cognitive impairment in mice by targeting increased cytokine levels with a small molecule experimental therapeutic. *J Neuroinflammation*. 12, 69. [PubMed: 25886256]
- Bachstetter AD, Zhou Z, Rowe RK, Xing B, Goulding DS, Conley AN, Sompol P, Meier S, Abisambra JF, Lifshitz J, Watterson DM, Van Eldik LJ, 2016 MW151 Inhibited IL-1beta Levels after Traumatic Brain Injury with No Effect on Microglia Physiological Responses. *PLoS One*. 11, e0149451. [PubMed: 26871438]
- Carbonell WS, Grady MS, 1999 Regional and temporal characterization of neuronal, glial, and axonal response after traumatic brain injury in the mouse. *Acta Neuropathol*. 98, 396–406. [PubMed: 10502046]
- Cherry JD, Tripodis Y, Alvarez VE, Huber B, Kiernan PT, Daneshvar DH, Mez J, Montenegro PH, Solomon TM, Alosco ML, Stern RA, McKee AC, Stein TD, 2016 Microglial neuroinflammation contributes to tau accumulation in chronic traumatic encephalopathy. *Acta Neuropathol Commun*. 4, 112. [PubMed: 27793189]
- Cole JT, Yarnell A, Kean WS, Gold E, Lewis B, Ren M, McMullen DC, Jacobowitz DM, Pollard HB, O'Neill JT, Grunberg NE, Dalgard CL, Frank JA, Watson WD, 2011 Craniotomy: true sham for traumatic brain injury, or a sham of a sham? *J Neurotrauma*. 28, 359–69. [PubMed: 21190398]
- Cortez SC, McIntosh TK, Noble LJ, 1989 Experimental fluid percussion brain injury: vascular disruption and neuronal and glial alterations. *Brain Res*. 482, 271–82. [PubMed: 2706487]
- Dixon CE, Lyeth BG, Povlishock JT, Findling RL, Hamm RJ, Marmarou A, Young HF, Hayes RL, 1987 A fluid percussion model of experimental brain injury in the rat. *J Neurosurg*. 67, 110–9. [PubMed: 3598659]
- Faul M, Xu L, Wald MM, Coronado VG, 2010 Traumatic Brain Injury in the United States: Emergency Department Visits, Hospitalizations and Deaths 2002–2006. Vol., ed.eds. Centers for Disease Control and Prevention, National Center for Injury Prevention and Control, Atlanta, GA.
- Fenn AM, Gensel JC, Huang Y, Popovich PG, Lifshitz J, Godbout JP, 2014 Immune activation promotes depression 1 month after diffuse brain injury: a role for primed microglia. *Biol Psychiatry*. 76, 575–84. [PubMed: 24289885]
- Fenn AM, Skendelas JP, Moussa DN, Muccigrosso MM, Popovich PG, Lifshitz J, Eiferman DS, Godbout JP, 2015 Methylene blue attenuates traumatic brain injury-associated neuroinflammation and acute depressive-like behavior in mice. *J Neurotrauma*. 32, 127–38. [PubMed: 25070744]

- Fukuda K, Tanno H, Okimura Y, Nakamura M, Yamaura A, 1995 The blood-brain barrier disruption to circulating proteins in the early period after fluid percussion brain injury in rats. *J Neurotrauma*. 12, 315–24. [PubMed: 7473806]
- Grady MS, Charleston JS, Maris D, Witgen BM, Lifshitz J, 2003 Neuronal and glial cell number in the hippocampus after experimental traumatic brain injury: analysis by stereological estimation. *J Neurotrauma*. 20, 929–41. [PubMed: 14588110]
- Greer JE, McGinn MJ, Povlishock JT, 2011 Diffuse traumatic axonal injury in the mouse induces atrophy, c-Jun activation, and axonal outgrowth in the axotomized neuronal population. *J Neurosci*. 31, 5089–105. [PubMed: 21451046]
- Kabadi SV, Hilton GD, Stoica BA, Zapple DN, Faden AI, 2010 Fluid-percussion-induced traumatic brain injury model in rats. *Nat Protoc*. 5, 1552–63. [PubMed: 20725070]
- Kokiko-Cochran ON, Saber M, Puntambekar S, Bemiller SM, Katsumoto A, Lee YS, Bhaskar K, Ransohoff RM, Lamb BT, 2018 Traumatic Brain Injury in hTau Model Mice: Enhanced Acute Macrophage Response and Altered Long-Term Recovery. *J Neurotrauma*. 35, 73–84. [PubMed: 28859549]
- Lifshitz J, Rowe RK, Griffiths DR, Evilsizor MN, Thomas TC, Adelson PD, McIntosh TK, 2016 Clinical relevance of midline fluid percussion brain injury: Acute deficits, chronic morbidities and the utility of biomarkers. *Brain Inj*. 30, 1293–1301. [PubMed: 27712117]
- Love MI, Huber W, Anders S, 2014 Moderated estimation of fold change and dispersion for RNA-seq data with DESeq2. *Genome Biol*. 15, 550. [PubMed: 25516281]
- Lyeth BG, 2016 Historical Review of the Fluid-Perussion TBI Model. *Front Neurol*. 7, 217. [PubMed: 27994570]
- McIntosh TK, Noble L, Andrews B, Faden AI, 1987 Traumatic brain injury in the rat: characterization of a midline fluid-percussion model. *Cent Nerv Syst Trauma*. 4, 119–34. [PubMed: 3690695]
- Ramlackhansingh AF, Brooks DJ, Greenwood RJ, Bose SK, Turkheimer FE, Kinnunen KM, Gentleman S, Heckemann RA, Gunanayagam K, Gelosa G, Sharp DJ, 2011 Inflammation after trauma: microglial activation and traumatic brain injury. *Ann Neurol*. 70, 374–83. [PubMed: 21710619]
- Schurman LD, Smith TL, Morales AJ, Lee NN, Reeves TM, Phillips LL, Lichtman AH, 2017 Investigation of left and right lateral fluid percussion injury in C57BL6/J mice: In vivo functional consequences. *Neurosci Lett*. 653, 31–38. [PubMed: 28527714]
- Vink R, Mullins PG, Temple MD, Bao W, Faden AI, 2001 Small shifts in craniotomy position in the lateral fluid percussion injury model are associated with differential lesion development. *J Neurotrauma*. 18, 839–47. [PubMed: 11526990]
- Witcher KG, Bray CE, Dziabis JE, McKim DB, Benner BN, Rowe RK, Kokiko-Cochran ON, Popovich PG, Lifshitz J, Eiferman DS, Godbout JP, 2018 Traumatic brain injury-induced neuronal damage in the somatosensory cortex causes formation of rod-shaped microglia that promote astrogliosis and persistent neuroinflammation. *Glia*. 66, 2719–2736. [PubMed: 30378170]

Highlights

- Midline and lateral FPI model aspects of focal and diffuse TBI in rodents
- Midline and lateral FPI induce similar acute cell infiltration and cytokine expression
- Midline and lateral FPI induced divergent sub-acute inflammatory responses
- Lateral FPI induced more cortical loss and greater Iba1+ immunoreactivity 7 dpi
- Midline FPI caused persistent neuroinflammatory gene expression 7 dpi

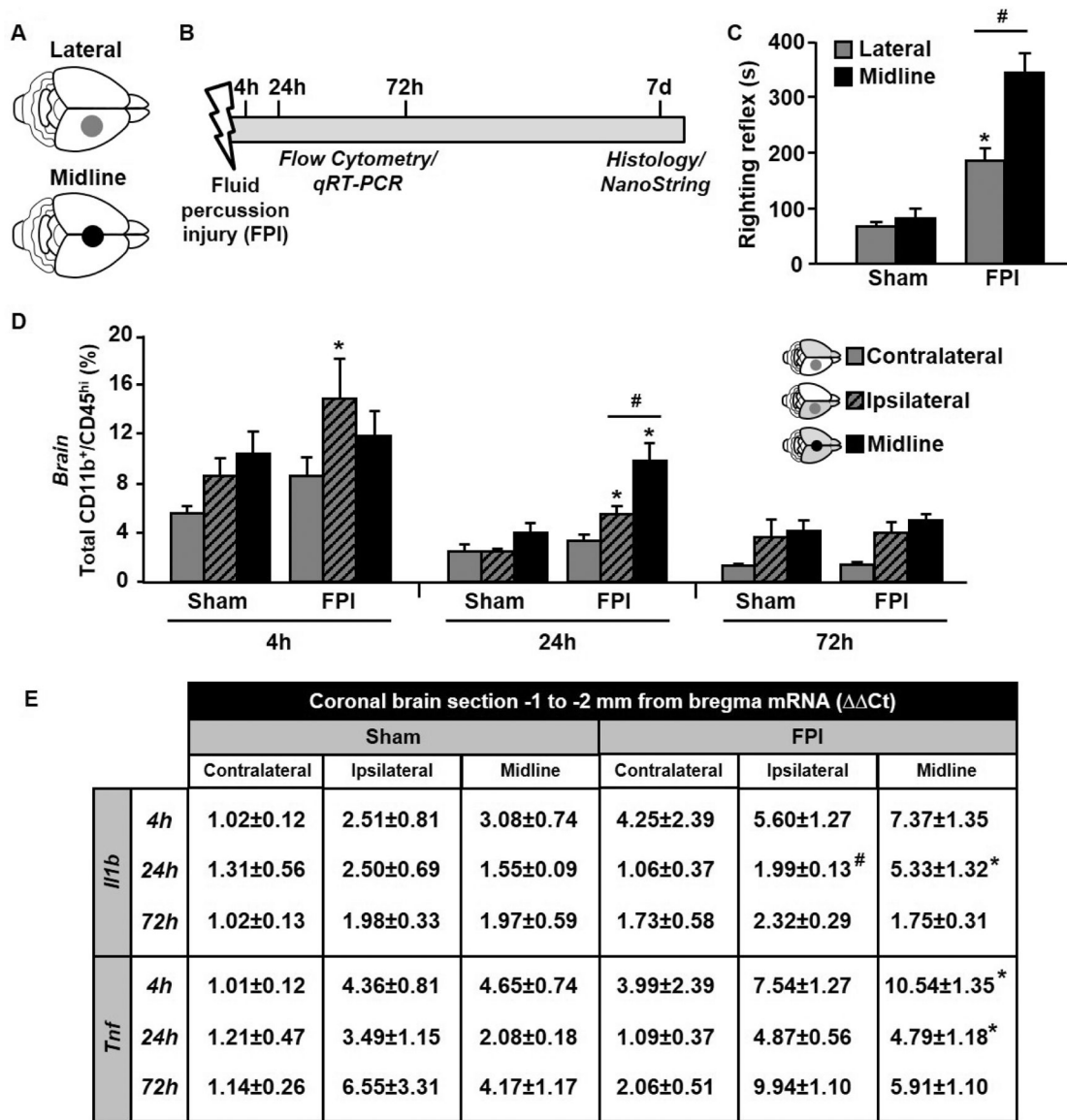


Figure 1. Midline FPI induces prolonged righting reflex but similar acute inflammatory response compared to lateral FPI.

Adult C57BL/6 mice were sham-injured or subjected to midline FPI applied -0.5 to -3.5 mm from bregma and midpoint along the sagittal suture (black circle) or lateral FPI applied -0.5 to -2.5 mm from bregma and midpoint 2.5 mm lateral to the sagittal suture (grey circle) (A). (B) Timeline of experimental procedures. In brief, 4, 24, or 72 hours post-injury (hpi), mice were sacrificed and brain-associated leukocytes were quantified by flow cytometry. In the same mice, a representative coronal brain section -1 to -2 mm from bregma was collected and qRT-PCR was used to quantify cytokine gene expression. (C) Average time to self-right following midline or lateral FPI. (D) Average number of CD11b⁺/CD45^{hi} infiltrating myeloid cells in the cortex 4, 24, and 72 hpi. (E) *Ilf1b* and *Tnf* gene expression relative to the contralateral hemisphere of sham mice. Data are expressed as average \pm standard error of the mean. Different letters indicate means are statistically

different. * denotes $p < 0.05$ compared to corresponding sham-injured control. # denotes $p < 0.05$ between midline FPI and ipsilateral cortex after lateral FPI.

Author Manuscript

Author Manuscript

Author Manuscript

Author Manuscript

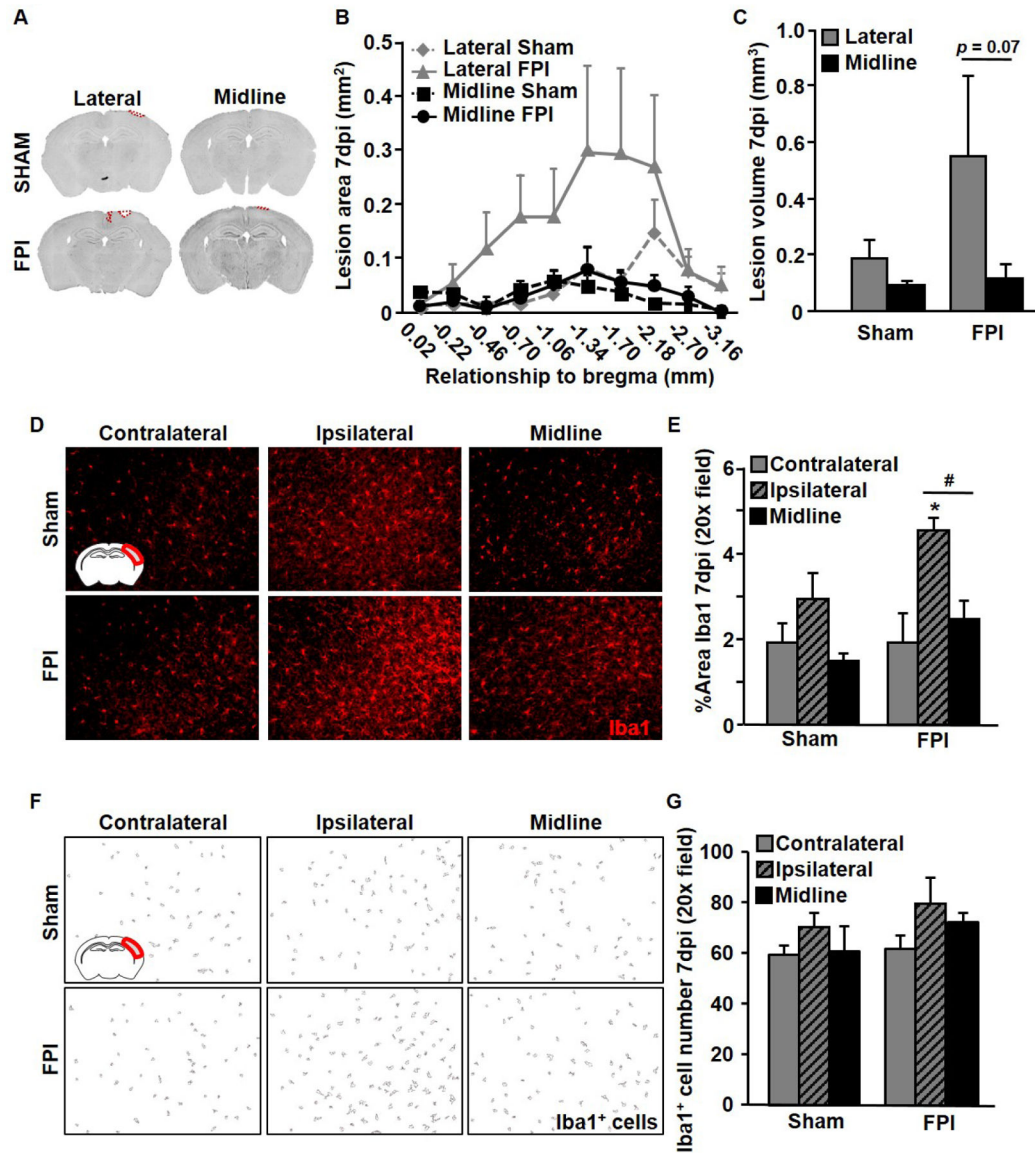


Figure 2. Lateral FPI causes greater cortical lesion volume and microglial morphological shift compared to midline FPI 7 DPI.

Adult C57BL/6 mice were sham-injured or subjected to midline or lateral FPI. Mice were sacrificed 7 dpi, perfuse-fixed, and coronal sections were used for lesion analysis and immunohistochemistry. (A) Representative coronal sections from midline and lateral FPI with lesion area highlighted in red. (B) Average lesion area in mm² at each coordinate measured for midline and lateral FPI and corresponding sham-injured controls. (C) Average total lesion volume across the same brain coordinates (mm³). (D) Representative images of Iba1 labeling in the cortex (inset). (E) Average Iba1+ percent area in the cortex. (F) Representative images from particle analysis of Iba1+ cells in the primary somatosensory cortex of the right brain hemisphere. (G) Average number of Iba1+ cells per experimental groups at 7 DPI.

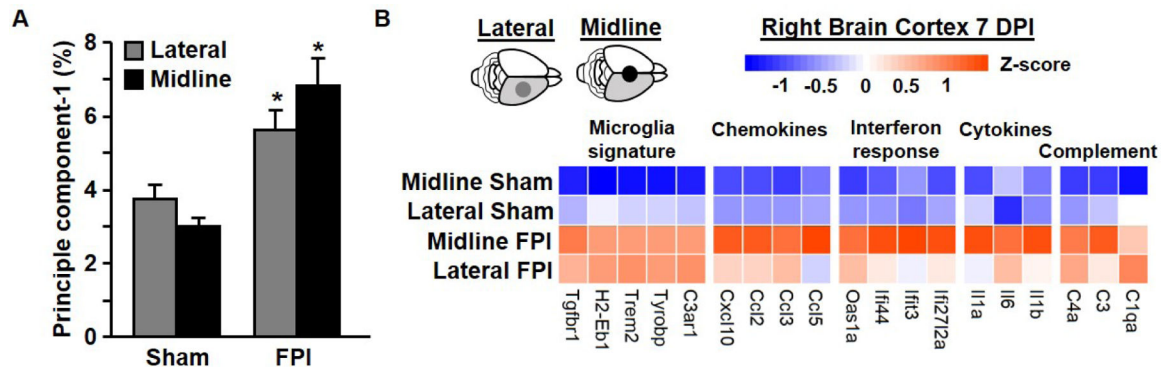


Figure 3. Midline FPI exaggerates cortical inflammatory gene expression compared to lateral FPI 7 DPI.

Adult C57BL/6 mice were sham-injured or subjected to midline or lateral FPI. Mice were sacrificed 7 dpi and the cortex from the right brain hemisphere was dissected. Cortical mRNA was extracted following midline and lateral FPI as well as sham injured controls. Copy number of immune/inflammatory genes was determined by NanoString nCounter assay and normalized to GAPDH housekeeping gene. (A) Average value of principle component analysis. (B) Heatmap shows average gene expression for selected genes, with blue representing lowest expression and orange reflecting highest expression for each gene. Values are expressed as average \pm standard error of the mean. * denotes $p < 0.05$ compared to corresponding sham-injured control. # denotes $p < 0.05$ between midline FPI and ipsilateral cortex after lateral FPI.